Hindawi Publishing Corporation
International Journal of Antennas and Propagation
Volume 2015, Article ID 278160, 9 pages
http://dx.doi.org/10.1155/2015/278160

Research Article

Linear Array Design with Switched Beams for Wireless Communications Systems

Vinícius Ludwig-Barbosa,[1] Edson Schlosser,[2] Renato Machado,[1,3] Filipe Guterres Ferreira,[2] Sabrina Müller Tolfo,[2] and Marcos Vinício Thomas Heckler[2]

[1]*Universidade Federal de Santa Maria, 97105-900 Santa Maria, RS, Brazil*
[2]*Universidade Federal do Pampa, 97546-550 Alegrete, RS, Brazil*
[3]*Blekinge Institute of Technology, 371 79 Karlskrona, Sweden*

Correspondence should be addressed to Vinícius Ludwig-Barbosa; viniciuslbar@mail.ufsm.br

Received 19 September 2014; Revised 30 March 2015; Accepted 3 April 2015

Academic Editor: Wenhua Chen

This paper presents an analysis for optimal design of switched beamforming applied to a linear array for wireless communication systems. The beam switching scheme provides coverage of a given sector in azimuth and controls the sidelobe level simultaneously. The analysis was developed considering arrays composed of Quasi-Yagi elements. The model assumes a user moving in the azimuthal direction under a constant velocity and with an estimation of the signal-to-noise ratio (SNR) at the mobile user (MU). The radio base station applies the beam that yields the best performance during transmission. The decision is based on the feedback information received from the MU. The goal of the analysis is to determine the best trade-off between the array size and number of feedback bits necessary to maximize the SNR at the receiver. The results show that a compromise between the number of beam-pointing directions and the array size should be taken into consideration for a wireless communication system design.

1. Introduction

The evolution of wireless communication systems is notorious. The amount of services available to mobile users is enormous and the quality of service should be great in the same proportion. During the last decades, different techniques were proposed aiming at improving the system performance and its capabilities of providing services to a greater number of subscribers. The cellular system, for example, has evolved through many generations to improve the quality of service (QoS), data rate, system reliability, and robustness [1].

Antennas and arrays have played an important role along this evolution. Several designs and techniques were applied to wireless communications in order to improve the system performance, such as MIMO systems combined with antenna array and smart antenna concepts [2–4].

As a simpler alternative to smart antennas, an array with switched beams is an interesting technique to be explored. This approach relies on the use of predefined beam-pointing directions that can be set at any time as it is required. The lower level of complexity compared to adaptive beamforming is an important advantage of this technique. It is based on a quantized version of space, in contrast to the continuous space that is covered by fully smart antennas.

In addition, the radiation pattern of the antenna array is an important aspect due to the necessity of suppressing the radiated power towards unwanted directions. In order to deal with this challenge, some methods of pattern synthesis are used to provide the excitation current of each antenna that composes the array. Fourier Transform, Woodward-Lawson, and Dolph-Chebyshev could be mentioned as the most common methods applied to fit the desired radiation pattern and control sidelobe level (SLL) [5, 6]. However, these techniques generally do not take mutual coupling into account. This can be a limitation for accurate beamforming.

In this paper, the study of arrays with switched beams is investigated. The beams have been synthesized by an

approach that combines genetic algorithm (GA) and sequential quadratic programming (SQP). This approach includes mutual coupling between the array elements in the synthesis process. These two techniques have been chosen for the present work because they combine both global and local optimization algorithms and they have been used successfully for other beam shaping problems [2]. The analysis presented in this paper provides a better insight on how to design linear array with switched beams, seeking for an optimal compromise between the number of antennas and beams for the antenna array at the radio base station (RBS) aiming at maximizing the signal-to-noise ratio (SNR) at the receiver. This analysis is important to improve the performance of a wireless communication system, as investigated in [7–9].

The analysis is applied on an array of Quasi-Yagi elements, which are composed basically of a fed structure (driver) and directors (parasitics). Parasitic antennas have large application combined with beam switching technique [10–12]. In all these cases, different radiation patterns are produced by commuting PIN diodes and modifying the electrical length of the parasitic elements. The advantages and feasibility of Quasi-Yagi elements applied on antennas arrays are highlighted in [13–15]. In [14], Cai et al. present a two-element array producing only one beam while [15] presents an array of 4 elements and 4 different radiation patterns in distinguished directions. In both cases, the patterns are not optimized concerning sidelobe levels. In addition, the array presented in [15] is implemented with microstrip delay lines to produce the appropriated phase shifts. Either in [15] or in PIN diode-based applications, the beam-switched arrays have their beam steering capacity limited by their structure. In this context, we present an analysis for optimal design of Quasi-Yagi beam-switched linear array, digitally controlled, to yield a coverage of a given azimuth sector. Further, it must reach the best SNR by taking into account the trade-off between array size and feedback quantization. Since the array is digitally controlled, the number of beam-steering and directions are easily adapted for different scenarios. This characteristic makes the array more flexible and less dependent on its layout structure as for the case of integrating shift delay lines and embedded components into the array structure.

The paper is organized as follows. Section 2 presents the system model considered in this analysis. In Section 3, the main characteristics of Quasi-Yagi antennas are presented along with the model specifications applied in this paper. The theoretical background on optimization algorithms for array synthesis is addressed in Section 4. In Section 5, the array with switched beam for wireless communications system applications is presented. Section 6 presents the simulation results, which are used to evaluate different sets of switched beams. Finally, Section 7 presents the conclusions and some final remarks.

2. System Model

The system model considered in this paper is composed of a RBS, where a linear antenna array is installed on, and a mobile user (MU), which is moving in the azimuthal direction assuming a constant radial distance from the radio station, as shown in Figure 1. This scenario was chosen to simplify the analysis, reducing the amount of variables involved in the problem, and to emphasize the movement of the MU toward the azimuthal direction. This enforces the system to switch between the available beams as long as it is required.

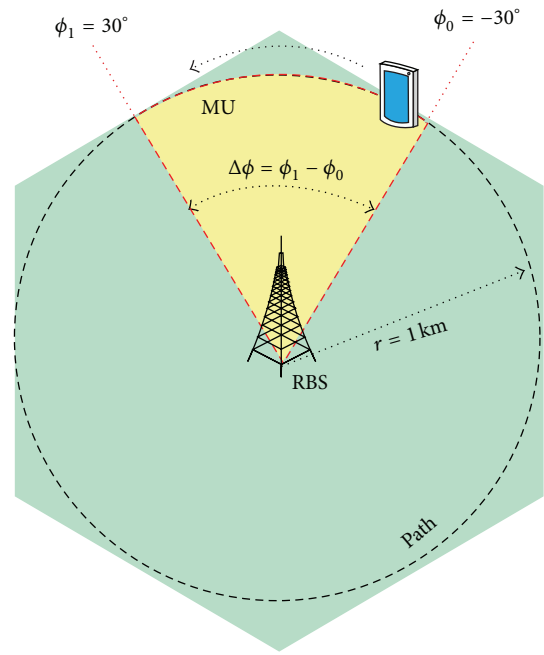

Figure 1: Mobile user scenario. The user moves with a uniform speed with constant radial distance from the RBS.

In the next subsections, the mathematical formulation used to model the signal properties and the relation between the transmitted and received signals is described.

2.1. Mobile User. The mobile terminal is assumed to be a user walking with a uniform speed of 6 km/h. The radial distance between MU and RBS is constant and equals 1 km, as depicted in Figure 1. The transmitting antenna array is considered to be sectorized [16] and its coverage is within −30 and 30 degrees. The MU model considered in this paper is the well-known uniform circular motion (UCM) [17], which suits the characteristics of the scenario under analysis. The equations are presented as follows:

$$v = \omega r, \tag{1}$$

where v is the linear speed and

$$\omega = \frac{\Delta\phi}{t} \tag{2}$$

is the angular velocity. The term $\Delta\phi$ is given in radians and is defined by

$$\Delta\phi = \phi_1 - \phi_0 = \frac{\Delta s}{r}, \tag{3}$$

where ϕ_1 and ϕ_0 are the limits of the coverage area, Δs is the walking distance, and r is the radial distance between RBS and MU.

2.2. Path Loss Model. The power received by the MU is calculated by using the free-space loss model (Friis equation) combined with the log-distance path loss model [18, 19]. Friis equation estimates fading between the RBS and the user and consequently the received power at the mobile terminal. The log-distance path loss model adds the urbanization effects to the losses. The free-space loss model is given by

$$P_L = 10\log\frac{P_r}{P_t} = 10\log\left[\mathrm{PLF}\frac{G_t(\theta_t,\phi_t)\,G_r(\theta_r,\phi_r)\,\lambda^2}{(4\pi)^2\,r^2}\right], \quad (4)$$

where PLF is the polarization loss factor, P_L is the total loss between RBS and MU (in dB), P_t is the transmitted power (in Watts), P_r is the received power (in Watts), G_t and G_r stand for the realized gains of the transmit (RBS) and receive (MU) antennas, respectively, and λ is the carrier wavelength in free space. The term r is the straight distance between the RBS and MU. The gains G_t and G_r take into account the reflection coefficient at the inputs of each antenna [20].

The losses caused by the urbanization effects can be computed by

$$L_{\mathrm{dB}}(d) = L(d_o) + 10n\log\left(\frac{r}{r_o}\right), \quad (5)$$

where r_o is a reference distance and n is the loss exponent. In this paper, we consider $r_o = 100$ m as a reference distance and $n = 4$, considering urban building effects.

Finally, the received power is given by

$$P_r\,(\mathrm{dBm}) = P_t\,(\mathrm{dBm}) - P_L\,(\mathrm{dB}) - L_{\mathrm{dB}}(d). \quad (6)$$

In this system model, it is assumed that the received signal at the MU is contaminated with a Gaussian noise with zero mean and variance N_0. Therefore, the SNR (dB) at the receiver is defined as

$$\mathrm{SNR}\,(\mathrm{dB}) = P_r\,(\mathrm{dBm}) - N_0\,(\mathrm{dBm}). \quad (7)$$

3. Quasi-Yagi Antennas

The Quasi-Yagi antenna gathers good features of printed and Yagi-Uda antennas. It has a low-profile structure, which allows installing it easily on the RBS or integrating it into an antenna array. In addition, the Quasi-Yagi antennas can be built using only one laminate, so that it can be considered a cost-effective solution for mass production.

A Quasi-Yagi antenna has been designed to operate with broadband centered at 2.4 GHz. The antenna has been built using an FR4 laminate with the following characteristics: dielectric constant $\varepsilon_r = 4.1$, loss tangent $\tan\delta = 0.02$, and laminate thickness $h = 1.58$ mm. Figure 2 presents the antenna prototype, which is composed of one active dipole and one director. The balun is implemented in microstrip technology and is used to provide a 180-degree phase shift between the two terminals of the active dipole. The antenna dimensions are listed in Table 1.

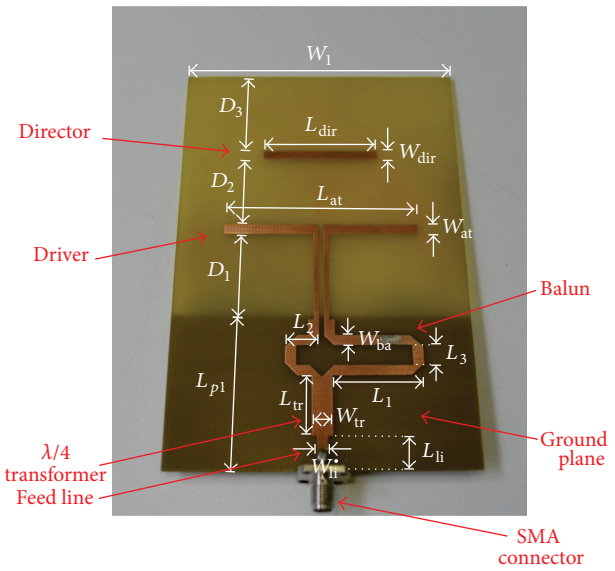

Figure 2: The prototype of the Quasi-Yagi antenna designed and used in this work.

Table 1: Parameters dimensions of the Quasi-Yagi antenna.

Parameter	Dimension (mm)
$L_{\mathrm{li}}, W_{\mathrm{li}}$	8.74, 2.86
$L_{\mathrm{tr}}, W_{\mathrm{tr}}$	16, 5.4
L_1	23.96
L_2	6.9
L_3	5.4
W_{ba}	2.86
L_{p1}, W_1	41.22, 80
D_1	24.5
D_2	20
$L_{\mathrm{at}}, W_{\mathrm{at}}$	54, 3
$L_{\mathrm{dir}}, W_{\mathrm{dir}}$	33.15, 3
L_{sub}	120

Figure 3 shows a comparison between simulated and measured curves for the reflection coefficient at the antenna input. One can see that good matching is achieved in the frequency range of 1.93–2.76 GHz considering the criterion of reflection coefficient lower than −10 dB. The reflection coefficient at 2.4 GHz satisfies this criterion for both the simulated and measured curves.

Figures 4 and 5 show calculated radiation patterns in the H- (azimuth) and E-planes (elevation). The gain at 2.4 GHz is 5.24 dBi, which is a good value considering that the antenna has been built on an FR4 laminate. An analysis of the variation of gain inside the band 1.93–2.76 GHz showed that the maximum gain achieved is 6.0 dBi at 2.76 GHz. The gain decreases for lower frequencies. The criterion assumed to determine the gain bandwidth was to consider a maximum variation of 3 dB related to the gain at 2.76 GHz, which is verified to occur at 2.01 GHz. Therefore, taking into consideration both criteria for reflection coefficient and gain variations

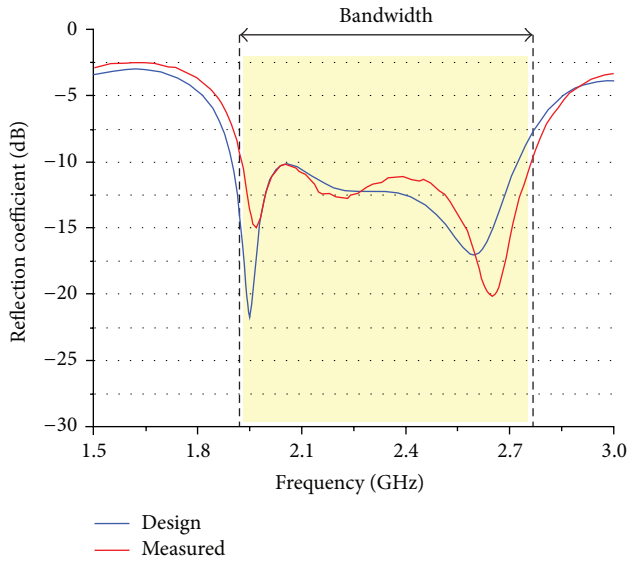

Figure 3: Comparison between simulated and measured results for the reflection coefficient at the antenna input.

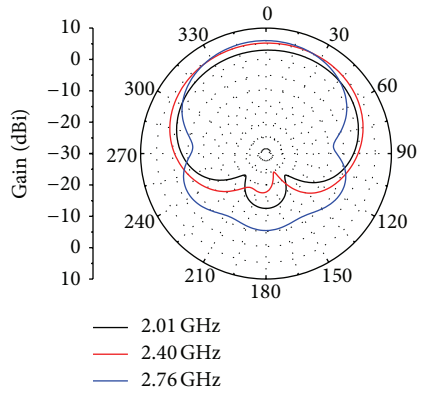

Figure 4: Radiation pattern in the H-plane (azimuth).

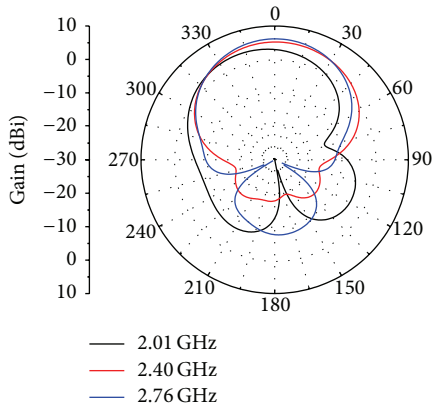

Figure 5: Radiation pattern in the E-plane (elevation).

over the frequency, the antenna operating bandwidth is 2.01–2.76 GHz.

4. Array Synthesis

Algorithms of pattern synthesis are powerful tools to control radiation pattern of an antenna array. These tools calculate the magnitudes and phases that should be applied to each array element in a way that parameters like half-power beamwidth, direction of the main beam, and sidelobe levels reach constraint values. There are some traditional algorithms, such as the Fourier Transform technique that do not produce satisfactory results when complex patterns are specified, unless a large number of elements are considered. Depending on the design needs, this may be a disadvantage, since the larger the array is, the more complex its construction is. The well-known Dolph-Chebyshev technique has good performance for SLL control, but it is limited to arrays composed of isotropic elements.

The complex coefficients for the antenna arrays considered in this paper are calculated by using two combined optimization methods: the genetic algorithm (GA) [21, 22] and the sequential quadratic programming (SQP) [23]. The GA is a method based on the evolution of an initial population that is generated randomly and is used to generate new populations. In the GA, the new individuals are expected to be closer and closer to the optimum solution for the optimization problem, until all the requirements are fulfilled. In the current implementation of GA, each individual is treated as a vector with its components standing for the magnitudes and phases of the currents that should be impressed at the array elements, as given by

$$\mathbf{I_j} = \left[\left|I_1\right| \ \angle\delta_1 \cdots \left|I_i\right| \ \angle\delta_i \cdots \left|I_N\right| \ \angle\delta_N\right], \tag{8}$$

where $\mathbf{I_j}$ stands for the jth individual in a population and $|I_i|$ and $\angle\delta_i$, $i = 1 \cdots N$, are the magnitude and phase of the current to be impressed at the ith array element, respectively. By looking at (8), each individual is composed of $2N$ genes and represents a set of excitation currents that produce the radiation pattern $\vec{E}_{\text{array}}(\phi)$. This pattern is a candidate solution for the synthesis problem.

In order to assess whether the pattern $\vec{E}_{\text{array}}(\phi)$ fulfills the imposed requirements, every individual is assigned with a fitness value based on the error function, which is calculated by [2]

$$g(\phi) = F(\phi) - \left|\vec{E}_{\text{array}}(\phi)\right|, \quad \phi \in [0^\circ, 180^\circ], \tag{9}$$

where $g(\phi)$ is the error between the specified pattern $F(\phi)$ and the calculated pattern $\vec{E}_{\text{array}}(\phi)$. The term $\phi \in [0^\circ, 180^\circ]$ is the angular interval in the azimuth plane in which the synthesis is done. A measure on how close the pattern corresponding to a given individual is to the specified pattern is achieved by the definition of a fitness value, which is calculated by

$$\text{fitness} = \frac{1}{L}\sum_{i=1}^{L}\left|g(\phi_i)\right|^2, \tag{10}$$

where L is the number of samples within the angular region under optimization. For every population, the fitness is calculated for every individual. The process of evolution runs until a predefined maximum number of generations are reached or until the specification for the fitness value is satisfied.

New populations are generated by selecting the individuals that present the best fitness values, by crossings of the individuals of a previous generation and by means of mutation. This last operation is important to avoid that GA converges to local minima. These are standard operations of the classical GA algorithm. Detailed information about them can be found in [21].

For the synthesis of a shaped pattern, the GA could be run until all the specifications are fulfilled. However, depending on how hard the specifications are, it may take several iterations and long computing time for the method to converge. In order to accelerate the synthesis process, the proposed approach considers running GA only for a predefined number of iterations (evolutions), so as to obtain an initial estimation of the coefficients. Even without any estimate for the currents to initialize the synthesis, this strategy is successful because GA is a global-search algorithm.

After the maximum number of generations is reached, the individual with the lowest fitness value is selected and used to start the SQP. Finally, SQP is run as a local-search approach until a set of coefficients that synthesize the pattern according to a specified mask pattern is obtained.

In contrast to other more complex shaped patterns, whereby the synthesized pattern is fixed and must follow a specified contour, the most important requirements for arrays with switched beams are only the direction of the main beam ϕ_m and the maximum allowed sidelobe level SLL. Such a mask is illustrated in Figure 6, which is the graphical representation of $F(\phi)$ in (9). The rectangles describe the region of the sidelobes and the arrow is used to represent the direction of the main beam. The regions between the main beam and the sidelobes are left without restrictions.

The Quasi-Yagi antenna has been used to compose arrays with 2, 4, and 8 elements. The geometry of the model simulated in HFSS for the case of 8 antennas is shown in Figure 7, where the spacing between adjacent elements is uniform and equals $d = 0.5\lambda$. This value is a design trade-off, since mutual coupling increases as d is made smaller, whilst the level of the sidelobes becomes larger and more difficult to control if d is made larger than 0.5λ.

Since the simulator is based on the finite element technique, the mutual coupling between the antennas is taken into account. In order to allow the synthesis, the individual antenna patterns are calculated and exported from HFSS. This is done by exciting only one antenna at a time and by setting the excitation at the other ports to 0. This is done for every antenna that composes the array. Finally, the radiation pattern of the array $\vec{E}_{\text{array}}(\phi)$ is calculated by the weighted vector sum of the individual patterns, whereby the weights are the complex excitation coefficients (currents) calculated by the synthesis algorithm.

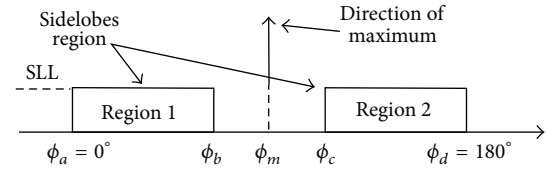

Figure 6: Mask applied for the synthesis of the switched beam arrays.

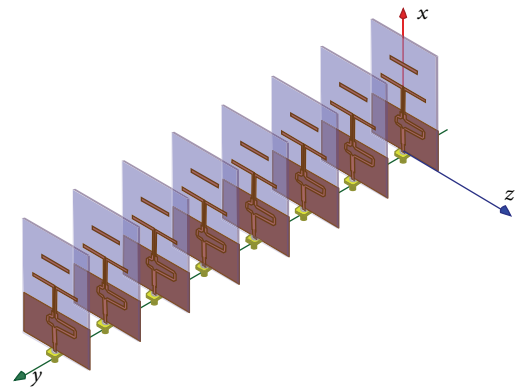

Figure 7: Simulated model of the array composed of 8 elements placed along the y-axis.

5. Beamforming Setup

In an ideal system, the transmitter at RBS should be able to follow the mobile user all the time in any direction inside the cell. However, in a real-world scenario, there is a feedback channel in between the MU and RBS, which can send only a few bits of feedback to the transmitter. It means that the feedback channel is quantized and, consequently, there must be a compromise between the array design, which includes the number of beam-pointing directions, and the SNR requirement.

The number of beams will depend on the amount of bits transmitted on the feedback channel and is governed by the constraints of the system. For example, if the feedback channel supports n bits, then the transmitter should be able to produce beams pointing to 2^n directions in the azimuthal plane.

Before each new transmission takes place, the RBS sends pilot bits with information on the available set of beams and the MU can estimate the SNR level that each pointing direction could yield. With this information, the receiver can evaluate which configuration is the most suitable and, therefore, could deliver the best performance during the current frame. Finally, the receiver feeds back the n bits containing the information (a label) correspondent to the beam-pointing direction (from a set of 2^n beam-pointing), which must be performed by the transmitter. This procedure is performed periodically and the RBS can upload the excitation coefficients (in the antenna array) for each new transmission frame, which makes the maximization of the SNR at the receiver possible.

The switching between the available beams occurs in the intersection point between adjacent beams. At this specific point, the minimum SNR value for the selected beam is reached. As a consequence, the QoS can decrease and only lower data rates become possible if the actual beam is kept during the transmission frame. Thus, at this moment, the switching to the adjacent beam occurs to provide higher gain in the direction of the MU. This approach guarantees that RBS applies the best beam-pointing to maximize the received SNR.

In the next section, simulation results are presented in order to evaluate the system performance for different array sizes and number of feedback bits. Based on the results, one can identify some trade-offs which should be kept in mind during the design of linear arrays with switched beams.

6. Simulation Results

This section presents some simulation results in order to assess the system performance for different array sizes and number of feedback bits. The SNR level is estimated based on the received power calculated using (6), which is sampled according to the speed of the user's motion. In this simulation, arrays of 2, 4, and 8 elements are considered. The beams for each array were synthesized using the mask depicted in Figure 6 by setting the values for ϕ_m so as to minimize the ripple and with SLL = 20 dB. The synthesis was run until the synthesized pattern fulfilled all the specifications given in Figure 6. The resulting sets of patterns are presented in Figure 10. For the simulations, the GA was set up for 40 individuals and for a maximal of 50 generations (iterations). The elapsed times for each case are the following: for the two-element array, 16 s; for the four-element array, 25 s; for the eight-element array, 37 s. The synthesis algorithm was run in MATLAB environment on computer with a core i7 processor with 3.4 GHz clock and 8 GB RAM.

The sets of patterns were tested for different design configurations, where the main motivation was to identify the best solution in terms of array size *versus* number of beam-pointing directions, where the latter is correlated with the number of feedbacks bits. For the simulations, the channel (user position) could be assumed to change randomly. However, it would not be a realistic assumption. Alternatively, a mathematical model can be used to simulate the user mobility within a cellular cell [24]. Therefore, in order to have a more realistic approach for the simulations, it is considered that a user moves at a constant velocity in the azimuthal direction, as illustrated in Figure 8. That is, there exists a constant angular velocity between receiver and transmitter. Thus, the system adaptivity is performed smoothly. The channel path loss model considered in the analysis is given by (6), which is described in more detail in Section 2.2. For all simulations, we assume that N_0 is −100 dBm (thermal noise) and the receiver has an omnidirectional antenna with G_r = 2 dBi.

The approach used to design the beam set (with 2^n steering inside the sector) provides approximately the same ripple variation between adjacent beams and between the sector boundaries, first/last beam and the coverage limits. This approach aims at increasing the QoS in the coverage area, thus keeping the SNR variation as low as possible [25]. The average ripple obtained for each system configuration is depicted in Table 2.

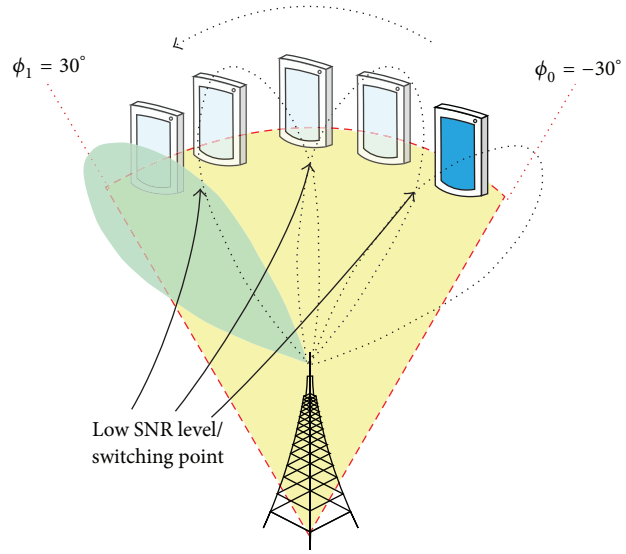

Figure 8: Array with switched beams on a RBS. The switching takes place in the intersection between adjacent beams.

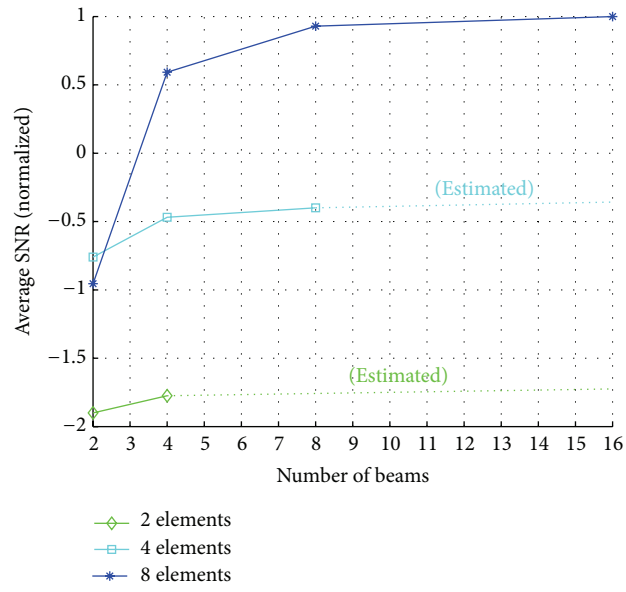

Figure 9: Average SNR as a function of the number of beam-pointing directions for different array sizes.

The ripple presented in Table 2 is basically dependent on the beamwidth. Arrays with few beams already yield low ripple due to broad beamwidth. This is clearly demonstrated by the two-element array. Larger arrays produce narrower beams. Consequently, more beam-pointing directions are required to reach low ripple levels. The worst-case ripple is around 15 dB, when an array of eight elements is combined with 2 beams. This configuration should be avoided since it is

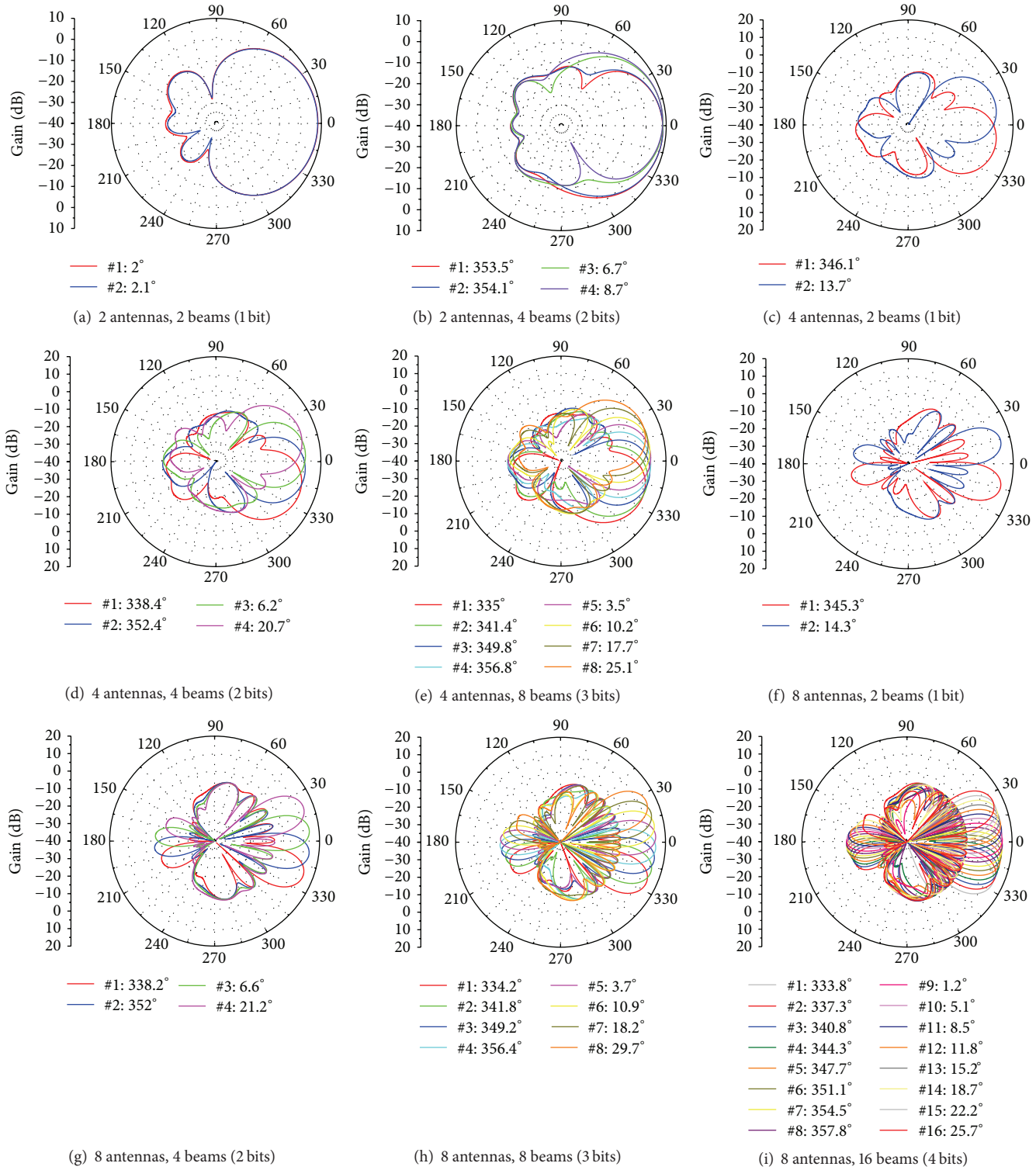

FIGURE 10: Gain patterns for the analyzed scenarios: linear arrays of 2, 4, and 8 elements. All patterns were synthesized with SLL = −20 dB below the main beam.

a combination of narrow beamwidth with a poor amount of beams.

From this point, it is possible to assess the system performance taking into account different configurations of array sizes × beam quantization levels. The power received at the MU was estimated according to the motion of the subscriber. This estimation was performed for each scenario under investigation.

Table 2: Average ripple between the maximum of lobe and the adjacent beam-pointing.

Array (elements, beams)	Ripple (dB)
(2, 2)	0.1
(2, 4)	0.1
(4, 2)	2.5
(4, 4)	0.7
(4, 8)	0.3
(8, 2)	15
(8, 4)	3
(8, 8)	0.8
(8, 16)	0.2

Figure 9 depicts the average normalized SNR for three array sizes, that is, arrays with 2, 4, and 8 elements. Considering the array with two elements (the green line with diamond dots), it is possible to realize that there is no gain (in a practical point of view) when the number of feedback bits (and the number of beam-pointing directions) is increased. For example, this system has 0.28 dB of gain when the number of feedback bits is increased from one to two. The relative gain (for $n+1$ compared to n bits) is even lower when the number of feedback bits is greater than 2. Based on those data and observing Figure 10, it is reasonable to discard this solution since the beamwidth of the two-element array is barely the same as that of the antenna designed (see Figure 4). As a result, using this array for beam switching applications is not advantageous.

When we compare the performance obtained by the array with four elements, it is notorious that the average SNR is higher than the one with two elements. For this case, one can see some advantage in exploring the feedback channel in order to improve the SNR level at the receiver. The SNR gain is approximately 0.65 dB from one over two feedback bits scenarios, which is already a significative result. Above this level of quantization ($n = 3$ or more), we can identify performance saturation.

Finally, the average SNR is improved in 5.22 dB when it is considered an array of eight elements with eight beam-pointing directions ($n = 3$ feedback bits). The increase in performance tends to become smaller and smaller when the number of feedback bits is greater than 3 (for this system configuration). As one can observe, the improvement made by the addition of feedback bits (or the number of beam-pointing directions) decreases as the number of feedback bits is increased (for all array sizes), giving an indication of performance saturation.

The differences among the analyzed arrays are mainly dependent on beamwidth and equivalent gain of each array. Larger arrays reach higher performances since the array equivalent gains are higher. However, the number of beams is more relevant since the ripple with few beams is greater, as observed in Table 2, and, basically, influenced by narrower beams. Therefore, an analysis such as the one presented in this paper is important and must be developed and evaluated to quantize the amount of beams in a given coverage area that guarantees maximization of SNR levels and, consequently, improvements in the system performance.

7. Conclusion

In this paper, a linear array design for wireless communication systems was proposed. The switched beamforming array scheme provides a coverage of a given angular area in the azimuthal plane and the sidelobe level is controlled simultaneously. The arrays evaluated in this paper are composed of two, four, and eight Quasi-Yagi elements. It was assumed that there is a user walking toward the azimuthal direction under a constant speed. The SNR at the receiver terminal remained as higher as possible according to the system configuration. The improvement made by the addition of feedback bits indicates performance saturation. The quantization of beam-pointing directions employed varies according to array size and should be taken into account for real-world systems in order to optimize the feedback channel usage. The analysis proves that an amount of beams equivalent to the number of elements (n elements and n beam-pointing directions) in a given array is a good trade-off in terms of array cost and SNR performance. An amount of beams bigger than the number of elements causes small improvements in the system performance, tending to saturation.

Conflict of Interests

This research does not have any competing interests concerning professional judgment, such as financial gain. All data shared on this paper has only academic interest and its reproduction is permitted unrestrictedly, since this original is properly cited.

Acknowledgments

This work was partially supported by the Coordination for the Improvement of Higher Education Personnel (CAPES/PROEX), Brazil, under Grant 1345 647, the National Council for Scientific and Technological Development (CNPq), Brazil, under Grants 211271-2013-6 and 306145/2013-8, the Swedish-Brazilian Research and Innovation Centre (CISB), and Saab AB.

References

[1] I. F. Akyildiz, D. M. Gutierrez-Estevez, and E. C. Reyes, "The evolution to 4G cellular systems: LTE-advanced," *Physical Communication*, vol. 3, no. 4, pp. 217–244, 2010.

[2] E. R. Schlosser, M. V. T. Heckler, C. Lucatel, M. Sperandio, and R. Machado, "Synthesis of linear antenna array for 4G mobile communication systems," in *Proceedings of the 15th SBMO/IEEE MTT-S International Microwave and Optoelectronics Conference (IMOC '13)*, pp. 1–5, August 2013.

[3] A. P. Gorbachev and V. M. Egorov, "A modified planar quasi-Yagi antenna for wireless communication applications," *IEEE Antennas and Wireless Propagation Letters*, vol. 8, pp. 1091–1093, 2009.

[4] M. Fernandes, A. Bhandare, C. Dessai, and H. Virani, "A wideband switched beam patch antenna array for LTE and Wi-Fi," in *Proceedings of the IEEE India Conference (INDICON '13)*, pp. 1–6, December 2013.

[5] W. P. M. N. Keizer, "Fast low-sidelobe synthesis for large planar array antennas utilizing successive fast fourier transforms of the array factor," *IEEE Transactions on Antennas and Propagation*, vol. 55, no. 3, pp. 715–722, 2007.

[6] M. D. Migliore, "MIMO antennas explained using the Woodward-Lawson synthesis method," *IEEE Antennas and Propagation Magazine*, vol. 49, no. 5, pp. 175–182, 2007.

[7] L. G. U. Garcia, M. A. Ingale, P.-H. Michaelsen, K. I. Pedersen, and P. E. Mogensen, "Impact of the pilot signal per beam on the ideal number of beams and capacity gain of switched beam forming for WCDMA," in *Proceedings of the IEEE 63rd Vehicular Technology Conference (VTC '06)*, vol. 6, pp. 2808–2812, July 2006.

[8] J. Ramiro-Moreno, K. I. Pedersen, and P. E. Mogensen, "Capacity gain of beamforming techniques in a WCDMA system under channelization code constraints," *IEEE Transactions on Wireless Communications*, vol. 3, no. 4, pp. 1199–1208, 2004.

[9] B. Allen and M. Beach, "On the analysis of switched-beam antennas for the WCDMA downlink," *IEEE Transactions on Vehicular Technology*, vol. 53, no. 3, pp. 569–578, 2004.

[10] Z. Imran and C. Panagamuwa, "Beam-switching planar parasitic antenna array," in *Proceedings of the Loughborough Antennas and Propagation Conference (LAPC '14)*, pp. 160–164, IEEE, Loughborough, UK, November 2014.

[11] J.-W. Baik, S. Pyo, T.-H. Lee, and Y.-S. Kim, "Switchable printed Yagi-Uda antenna with pattern reconfiguration," *ETRI Journal*, vol. 31, no. 3, pp. 318–320, 2009.

[12] C. Kittiyanpunya and M. Krairiksh, "Pattern reconfigurable printed Yagi-Uda antenna," in *Proceedings of the International Symposium on Antennas and Propagation (ISAP '14)*, pp. 325–326, December 2014.

[13] W. R. Deal, N. Kaneda, J. Sor, Y. Qian, and T. Itoh, "A new quasi-yagi antenna for planar active antenna arrays," *IEEE Transactions on Microwave Theory and Techniques*, vol. 48, no. 6, pp. 910–918, 2000.

[14] R.-N. Cai, M.-C. Yang, S. Lin, X.-Q. Zhang, X.-Y. Zhang, and X.-F. Liu, "Design and analysis of printed Yagi-Uda antenna and two-element array for WLAN applications," *International Journal of Antennas and Propagation*, vol. 2012, Article ID 651789, 8 pages, 2012.

[15] N. Nikolic and A. R. Weily, "Printed quasi-vagi antenna with folded dipole driver," in *Proceedings of the IEEE International Symposium on Antennas and Propagation and USNC/URSI National Radio Science Meeting (APSURSI '09)*, pp. 1–4, June 2009.

[16] J. Werner, J. Wang, A. Hakkarainen, M. Valkama, and D. Cabric, "Primary user localization in cognitive radio networks using sectorized antennas," in *Proceedings of the 10th Annual Conference on Wireless On-Demand Network Systems and Services (WONS '13)*, pp. 155–161, March 2013.

[17] D. Halliday, R. Resnick, and J. Walker, *Fundamentals of Physics*, John Wiley & Sons, 8th edition, 2007.

[18] T. Rappaport, *Wireless Communications: Principles and Practice*, Prentice Hall, 2nd edition, 2002.

[19] J. R. Fernandez, M. Quispe, G. Kemper, J. Samaniego, and D. Díaz, "Adjustments of log-distance path loss model for digital television in lima," *Proceedings of the 30th Simposio Brasileiro de Telecomunicações*, pp. 13–16, September 2012.

[20] IEEE, "IEEE standard for definitions of terms for antennas," IEEE Standard 145-2013, IEEE Standards Association, 2014, (Revision of IEEE Std 145-1993).

[21] J. M. Johnson and Y. Rahmat-Samii, "Genetic algorithms in engineering electromagnetics," *IEEE Antennas and Propagation Magazine*, vol. 39, no. 4, pp. 7–21, 1997.

[22] J. M. Johnson and Y. Rahmat-samii, "Genetic algorithm optimization and its application to antenna design," in *Proceedings of the IEEE Antennas and Propagation International Symposium*, vol. 1, pp. 326–329, June 1994.

[23] S. Koziel and S. Ogurtsov, "Linear antenna array synthesis using gradient-based optimization with analytical derivatives," in *Proceedings of the IEEE Antennas and Propagation Society International Symposium (APSURSI '12)*, pp. 1–2, Chicago, Ill, USA, July 2012.

[24] M. K. Karray, "User's mobility effect on the performance of wireless cellular networks serving elastic traffic," *Wireless Networks*, vol. 17, no. 1, pp. 247–262, 2011.

[25] M. Alasti, B. Neekzad, J. Hui, and R. Vannithamby, "Quality of service in WiMAX and LTE networks," *IEEE Communications Magazine*, vol. 48, no. 5, pp. 104–111, 2010.